EXTERIOR ORIENTATION OF LINE-ARRAY CCD IMAGES BASED ON QUATERNION SPHERICAL LINEAR INTERPOLATION

G. Jiang, T. Jiang *, H. Gong, X. Wang

Zhengzhou Institute of Surveying and Mapping, Information Engineering University, 66 Middle Longhai Road, Zhengzhou, Henan 450052 China - jianggw@vip.sina.com

KEY WORDS: Photogrammetry, Algorithm, CCD, Orientation, Correlation

ABSTRACT:

Since the exterior orientation elements of line-array CCD images are highly correlated, normal collinear equations that computing these elements are ill-posed and the error of the least square estimation is very large and the solution strongly depends on the initial value. For solving this problem, this paper puts forward an algorithm to compute the exterior orientation elements based on quaternion spherical linear interpolation. Firstly the quaternion is used to describe the attitude of the image, and then spherical linear interpolation is used to gain the attitude of any line in this algorithm, lastly a model of exterior orientation elements is build and is used in exterior orientation. Experimental results indicated that the method could effectively overcome the correlation problems of exterior orientation elements and the positioning accuracy is very high, and the reliability and stability of this algorithm are both independent of the initial values of exterior orientation elements.

1. INTRODUCTION

Line-array CCD images have stable geometric attributes, and it is quite meaningful to investigate the techniques of object orientation and stereo plotting by CCD images. However, line-array CCD images have a projection centre for each image line, and the orientation parameters of traditional linearization collinear equation are highly correlated. Thus, the equations to solve exterior orientation elements are greatly ill-posed. Least Square (LS) solutions, which are dependent on the initial values of exterior orientation elements, may have great errors, and the precision of orientation and mapping is greatly influenced (Wang, 1979; Qian, et.al, 1991).

Numerous investigations have been done by researchers on the precise computing the exterior orientation elements of line-array CCD images, and many methods to solve ill-posed problems are proposed (Qian, et al, 1991; Krupnik, 2000; Katiyar, et al.2003; Gupta, et al.1997), such as adding virtual error equations, combining great correlation items, iteratively solving the line and angle exterior orientation elements respectively, centralized criterion of coefficient and so on. Although the orientation precision is increased by these methods, the correlations and the ill-posed problems of normal equation are not solved. Consequently the precision is restricted. Subsequently, some scholars put forward some biased estimations (Guo, et al, 2003; Gui, et al. 2003; Wang, et al.2005), for example ridge estimation (including special and generalized ridge estimation), principal component analysis and stein estimation. However, there are various limitations in these biased estimations, and many works should be done to improve them. Moreover, for high resolution satellite CCD images (such as IKONOS images), rational function model, affine transformation method are investigated to objects positioning by many researchers (Okamoto, et al. 1999; Fraser, et al. 2002; Zhang, et al. 2004). For these methods, rigorous projection relationships between image coordinate system and ground coordinate system are not considered. This is the greatest advantage of these methods.

The ill-posed problems can be solved in two aspects. One is choosing the appropriate calculation methods. The other one is building appropriate math model. The above solutions just reduce the ill-posed problem from the calculation methods, without solving this problem in essential. In order to solve the ill-posed problem perfectly, this paper tries to build a model of exterior orientation elements using quaternion. Single image space resection based on quaternion is firstly studied and tested in Jiang's (Jiang, 2007) and Wang's (Wang, 2007) papers. Experimental results show that it can get correct solutions under a larger range of initial values than traditional way. However, frame photo is the research object in their paper, and their methods are not suit for processing the line-array CCD images. Liu's (LIU, 2008) paper extends the method to the bundle adjustment of airborne three-line images, and it behaves very well. However, his method is not suit for processing single line-array CCD images. So in this paper, when quaternion is used to describe the exterior orientation elements of the first and the last scan line of a line-array CCD image, we gain the quaternion attitude elements of any scan line through the method of quaternion spherical linear interpolation (SLERP). Then we put forward an algorithm of exterior orientation based on the quaternion SLERP (called quaternion algorithm). At last, we do some exterior orientation experiments by this algorithm.

The remainder of this paper is organized as follows: In Section 2, quaternion and quaternion spherical linear interpolation are briefly reviewed. Section 3 puts forward a SLERP model of exterior orientation elements based on quaternion, and an algorithm of exterior orientation using the above model is given. Experimental results and analysis are given in Section 4. Finally, Section 5 concludes the paper.

* Corresponding author.

2. QUATERNION SPHERICAL LINEAR INTERPOLATION

2.1 Quaternion representation of rotation

A quaternion is an ultra-complex number which expresses as $\dot{q} = q_0 + \boldsymbol{i}q_1 + \boldsymbol{j}q_2 + \boldsymbol{k}q_3$ (Zhang,1997),where q_0, q_1, q_2, q_3 are real numbers and $\boldsymbol{i}, \boldsymbol{j}, \boldsymbol{k}$ are so-called imaginary units whose products follow the rule $\boldsymbol{i}^2 = \boldsymbol{j}^2 = \boldsymbol{k}^2 = -1$, $\boldsymbol{jk} = -\boldsymbol{kj} = \boldsymbol{i}$, $\boldsymbol{ki} = -\boldsymbol{ik} = \boldsymbol{j}$, $\boldsymbol{ij} = -\boldsymbol{ji} = \boldsymbol{k}$. A quaternion also can be written as $\dot{q} = q_0 + \boldsymbol{q}$, where the number q_0 is called the real part and the sum $\boldsymbol{q} = \boldsymbol{i}q_1 + \boldsymbol{j}q_2 + \boldsymbol{k}q_3$ is called imaginary part. The vector form of quaternion is$\dot{q} = [q_0 \quad q_1 \quad q_2 \quad q_3]^{\mathrm{T}}$.The conjugate of a quaternion is $\dot{q}^* = q_0 - \boldsymbol{i}q_1 - \boldsymbol{j}q_2 - \boldsymbol{k}q_3$.The norm of a quaternion is$\|\dot{q}\| = \sqrt{\dot{q}\dot{q}^*}$.If the$\|\dot{q}\| = 1$, quaternion $\dot{q}$is called a unit quaternion.

The detailed discussion of quaternion is in Jiang's paper. Much of that is not exited in this paper. The rotation matrix which using the quaternion can be gained from the product rule of quaternion, the formula is as follow (JIANG,2007):

$$M = \begin{bmatrix} q_0^2 + q_1^2 - q_2^2 - q_3^2 & 2(q_1q_2 - q_0q_3) & 2(q_1q_3 + q_0q_2) \\ 2(q_2q_1 + q_0q_3) & q_0^2 - q_1^2 + q_2^2 - q_3^2 & 2(q_2q_3 - q_0q_1) \\ 2(q_3q_1 - q_0q_2) & 2(q_2q_3 + q_0q_1) & q_0^2 - q_1^2 - q_2^2 + q_3^2 \end{bmatrix} \tag{1}$$

When the order of the rotation axis is$Y - X - Z$, we can obtain the Euler angles $(\varphi, \omega, \kappa)$ from the above rotation matrix through the following formula.

$$\left.\begin{aligned} \varphi &= \tan^{-1}(\frac{-M_{13}}{M_{33}}) \\ \omega &= \tan^{-1}(-M_{23}) \\ \kappa &= \tan^{-1}(\frac{M_{21}}{M_{22}}) \end{aligned}\right\} \tag{2}$$

2.2 Quaternion Spherical Linear Interpolation

When quaternion is used to describe the image attitude, the spherical linear interpolation of quaternion can allow us to smoothly interpolate between two image attitudes (LIU, 2008). The principle of quaternion spherical linear interpolation is illustrated in figure 1. Given two unit quaternions $\dot{q}_1$、$\dot{q}_2$ and their inclination angle θ, the unit quaternion $\dot{q}(t)$ is on the arc which connected $\dot{q}_1$ and $\dot{q}_2$, and the inclination angle of $\dot{q}(t)$ and $\dot{q}_1$ is $t\theta$. So $\dot{q}(t)$ is given by:

$$\dot{q}(t) = C_1(t)\dot{q}_1 + C_2(t)\dot{q}_2 \tag{3}$$

Where, $C_1(t), C_2(t)$ are the coefficients, and t is the interpolative variable.

$$C_1(t) = \frac{\sin(1-t)\theta}{\sin\theta} \quad C_2(t) = \frac{\sin t\theta}{\sin\theta} \tag{4}$$

$$\begin{aligned} \theta &= \arccos(\dot{q}_1 \cdot \dot{q}_2) \\ &= \arccos(q_{10}q_{20} + q_{11}q_{21} + q_{12}q_{22} + q_{13}q_{23}) \end{aligned} \tag{5}$$

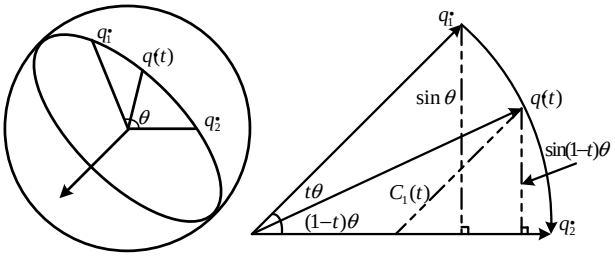

Figure 1. The outline of quaternion spherical linear interpolation

In this paper, we only give that how to obtain the expression of $C_1(t)$. From the geometry of figure 1, we can get two similarity triangles, so that.

$$\frac{C_1(t)}{\|\dot{q}_1\|} = \frac{\left\|\dot{q(t)}\right\| \sin(1-t)\theta}{\|\dot{q}_1\| \sin\theta}$$

$\dot{q}_1$ and $\dot{q}(t)$ are unit quaternions, $\|\dot{q}_1\| = \left\|\dot{q(t)}\right\| = 1$, so the we can obtain:

$$C_1(t) = \frac{\sin(1-t)\theta}{\sin\theta}$$

We can also obtain the expression of $C_2(t)$ similarly.

Using formula (4) in equation (3), the SLERP function of quaternion is given by

$$\dot{q}(t) = \frac{\sin(1-t)\theta}{\sin\theta}\dot{q}_1 + \frac{\sin t\theta}{\sin\theta}\dot{q}_2 \tag{6}$$

If we look upon two unit quaternions $\dot{q}_1$ and $\dot{q}_2$ as two points on the surface of a 4D sphere, quaternion SLERP will interpolate around the shortest arc that connects the two quaternions along the surface of the 4D sphere.

3. SOLUTION OF EXTERIOR ORIENTATION ELEMENTS

3.1 SLERP model of exterior orientation elements

In this paper, the projection center (i.e.,X_{Si}, Y_{Si}, Z_{Si}) in the elements of exterior orientation is expressed by linear interpolation, and the unit quaternion $\dot{q}_i$ is used to describe the angular elements, the quaternion attitude of any scan line is obtained by using SLERP.

The image projection of line-array CCD image is the line central projection, so the projection center of scan line i is given by:

$$\left.\begin{aligned} X_{Si} &= X_S + \dot{X}_S y_i \\ Y_{Si} &= Y_S + \dot{Y}_S y_i \\ Z_{Si} &= Z_S + \dot{Z}_S y_i \end{aligned}\right\} \tag{7}$$

Where X_{Si}, Y_{Si}, Z_{Si} is the projection center of scan line i; y_i is the measured y coordinate of the scan line i; X_S, Y_S, Z_S is the projection center of the centre line, and $\dot{X}_S, \dot{Y}_S, \dot{Z}_S$ are the coeffifients of change in the y direction.

When quaternion is used to describe the exterior orientation elements of the first and the last scan line of a line-array CCD image, the quaternion attitude of any scan line can be obtained by using SLERP.

$$\dot{q}_i = C_1(t)\dot{q}_1 + C_2(t)\dot{q}_2 \tag{8}$$

Where $\dot{q}_i$ is the quaternion attitude of any scan line; $\dot{q}_1$ and $\dot{q}_2$ are the quaternion attitude of the first and the last scan line; $C_1(t), C_2(t)$ is given by formula (4).

Using the vector expression of $\dot{q}_i$, $\dot{q}_1$ and $\dot{q}_2$ in formula (8), $\dot{q}_i$ is given by:

$$\begin{bmatrix} q_{i0} \\ q_{i1} \\ q_{i2} \\ q_{i3} \end{bmatrix} = \begin{bmatrix} C_1(t)q_{10} + C_2(t)q_{20} \\ C_1(t)q_{11} + C_2(t)q_{21} \\ C_1(t)q_{12} + C_2(t)q_{22} \\ C_1(t)q_{13} + C_2(t)q_{23} \end{bmatrix} \tag{9}$$

The interpolative variable t is given by:

$$t = \frac{i}{n} \qquad (0 < t < 1) \tag{10}$$

Where i is the row number of the scan line; n is the total scan line number of a view image.

3.2 Linearization of collinear equation with SLERP model

In the error equation of exterior orientation based on quaternion SLERP model, the unknown elements are (X_S,Y_S,Z_S,$\dot{X}_S$,$\dot{Y}_S$, $\dot{Z}_S$,q_{10},q_{11},q_{12},q_{13},q_{20},q_{21},q_{22},q_{23}). The following is about that how to linearize the collinear equation based on quaternion SLERP model.

In the line-array CCD image, we assume that f is known, and $(x_0, y_0) = (0, 0)$. For any GCP, the coordinates are known, $\mathrm{d}X = \mathrm{d}Y = \mathrm{d}Z = 0$. The linearization error equation is given by:

$$\left.\begin{aligned} v_x =& k_{11}\mathrm{d}X_{Si} + k_{12}\mathrm{d}Y_{Si} + k_{13}\mathrm{d}Z_{Si} \\ &+ k_{14}\mathrm{d}q_{i0} + k_{15}\mathrm{d}q_{i1} + k_{16}\mathrm{d}q_{i2} + k_{17}\mathrm{d}q_{i3} - l_x \\ v_y =& k_{21}\mathrm{d}X_{Si} + k_{22}\mathrm{d}Y_{Si} + k_{23}\mathrm{d}Z_{Si} \\ &+ k_{24}\mathrm{d}q_{i0} + k_{25}\mathrm{d}q_{i1} + k_{26}\mathrm{d}q_{i2} + k_{27}\mathrm{d}q_{i3} - l_y \end{aligned}\right\} \tag{11}$$

Where

$$\begin{aligned} k_{11} &= (a_{1i}f + a_{3i}x)/\bar{Z} & k_{21} &= a_{2i}f/\bar{Z} \\ k_{12} &= (b_{1i}f + b_{3i}x)/\bar{Z} & k_{22} &= b_{2i}f/\bar{Z} \\ k_{13} &= (c_{1i}f + c_{3i}x)/\bar{Z} & k_{23} &= c_{2i}f/\bar{Z} \\ k_{14} &= 2(f + x^2/f)q_{i2} & k_{24} &= -2(q_{i1}f + q_{i3}x) \\ k_{15} &= -2(f + x^2/f)q_{i3} & k_{25} &= 2(q_{i0}f + q_{i2}x) \\ k_{16} &= -2(f + x^2/f)q_{i0} & k_{26} &= -2(q_{i3}f + q_{i1}x) \\ k_{17} &= 2(f + x^2/f)q_{i1} & k_{27} &= 2(q_{i2}f + q_{i0}x) \end{aligned}$$

$$l_x = x - x', x' = -f(\bar{X}/\bar{Z})$$

$$l_y = 0 - y', y' = -f(\bar{Y}/\bar{Z})$$

$$\bar{X} = a_{1i}(X - X_{Si}) + b_{1i}(Y - Y_{Si}) + c_{1i}(Z - Z_{Si})$$

$$\bar{Y} = a_{2i}(X - X_{Si}) + b_{2i}(Y - Y_{Si}) + c_{2i}(Z - Z_{Si})$$

$$\bar{Z} = a_{3i}(X - X_{Si}) + b_{3i}(Y - Y_{Si}) + c_{3i}(Z - Z_{Si})$$

$$\begin{bmatrix} a_{1i} & b_{1i} & c_{1i} \\ a_{2i} & b_{2i} & c_{2i} \\ a_{3i} & b_{3i} & c_{3i} \end{bmatrix} =$$

$$\begin{bmatrix} q_{i0}^2 + q_{i1}^2 - q_{i2}^2 - q_{i3}^2 & 2(q_{i1}q_{i2} - q_{i0}q_{i3}) & 2(q_{i1}q_{i3} + q_{i0}q_{i2}) \\ 2(q_{i2}q_{i1} + q_{i0}q_{i3}) & q_{i0}^2 - q_{i1}^2 + q_{i2}^2 - q_{i3}^2 & 2(q_{i2}q_{i3} - q_{i0}q_{i1}) \\ 2(q_{i3}q_{i1} - q_{i0}q_{i2}) & 2(q_{i2}q_{i3} + q_{i0}q_{i1}) & q_{i0}^2 - q_{i1}^2 - q_{i2}^2 + q_{i3}^2 \end{bmatrix}$$

The differential equation of equation (7) is given by:

$$\left.\begin{aligned} \mathrm{d}X_{Si} &= \mathrm{d}X_S + y\mathrm{d}\dot{X}_S \\ \mathrm{d}Y_{Si} &= \mathrm{d}Y_S + y\mathrm{d}\dot{Y}_S \\ \mathrm{d}Z_{Si} &= \mathrm{d}Z_S + y\mathrm{d}\dot{Z}_S \end{aligned}\right\} \tag{12}$$

For the same reason, we can gain the differential expression of equation (9) considering that q_{i0},q_{i1},q_{i2},q_{i3} is the function of q_{10},q_{11},q_{12},q_{13} and q_{20},q_{21},q_{22},q_{23}.

$$\begin{aligned} \mathrm{d}q_{im} =& \frac{\partial q_{im}}{\partial q_{10}}\mathrm{d}q_{10} + \frac{\partial q_{im}}{\partial q_{11}}\mathrm{d}q_{11} + \frac{\partial q_{im}}{\partial q_{12}}\mathrm{d}q_{12} + \frac{\partial q_{im}}{\partial q_{13}}\mathrm{d}q_{13} \\ &+ \frac{\partial q_{im}}{\partial q_{20}}\mathrm{d}q_{20} + \frac{\partial q_{im}}{\partial q_{21}}\mathrm{d}q_{21} + \frac{\partial q_{im}}{\partial q_{22}}\mathrm{d}q_{22} + \frac{\partial q_{im}}{\partial q_{23}}\mathrm{d}q_{23} \\ & (m = 0, 1, 2, 3) \end{aligned} \tag{13}$$

In the equation (13), there are thirty-two deflection differential coefficients. Through math deduction, we can obtain the expression of these deflection differential coefficients simply. The following is the expression of the deflection differential coefficients for $\mathrm{d}q_{i0}$.

$$\left.\begin{aligned} \frac{\partial q_{i0}}{\partial q_{10}} &= \frac{\partial \theta}{\partial q_{10}}\left(\frac{\partial C_1(t)}{\partial \theta}q_{10} + \frac{\partial C_2(t)}{\partial \theta}q_{20}\right) + C_1(t) \\ \frac{\partial q_{i0}}{\partial q_{11}} &= \frac{\partial \theta}{\partial q_{11}}\left(\frac{\partial C_1(t)}{\partial \theta}q_{10} + \frac{\partial C_2(t)}{\partial \theta}q_{20}\right) \\ \frac{\partial q_{i0}}{\partial q_{12}} &= \frac{\partial \theta}{\partial q_{12}}\left(\frac{\partial C_1(t)}{\partial \theta}q_{10} + \frac{\partial C_2(t)}{\partial \theta}q_{20}\right) \\ \frac{\partial q_{i0}}{\partial q_{13}} &= \frac{\partial \theta}{\partial q_{13}}\left(\frac{\partial C_1(t)}{\partial \theta}q_{10} + \frac{\partial C_2(t)}{\partial \theta}q_{20}\right) \\ \frac{\partial q_{i0}}{\partial q_{20}} &= \frac{\partial \theta}{\partial q_{20}}\left(\frac{\partial C_1(t)}{\partial \theta}q_{10} + \frac{\partial C_2(t)}{\partial \theta}q_{20}\right) + C_2(t) \\ \frac{\partial q_{i0}}{\partial q_{21}} &= \frac{\partial \theta}{\partial q_{21}}\left(\frac{\partial C_1(t)}{\partial \theta}q_{10} + \frac{\partial C_2(t)}{\partial \theta}q_{20}\right) \\ \frac{\partial q_{i0}}{\partial q_{22}} &= \frac{\partial \theta}{\partial q_{22}}\left(\frac{\partial C_1(t)}{\partial \theta}q_{10} + \frac{\partial C_2(t)}{\partial \theta}q_{20}\right) \\ \frac{\partial q_{i0}}{\partial q_{23}} &= \frac{\partial \theta}{\partial q_{23}}\left(\frac{\partial C_1(t)}{\partial \theta}q_{10} + \frac{\partial C_2(t)}{\partial \theta}q_{20}\right) \end{aligned}\right\} \tag{14}$$

Where

$$\frac{\partial C_1(t)}{\partial \theta} = \frac{(1-t)\cos(1-t)\theta\sin\theta - \sin(1-t)\theta\cos\theta}{\sin^2\theta}$$

$$\frac{\partial C_2(t)}{\partial \theta} = \frac{t\cos t\theta\sin\theta - \sin t\theta\cos\theta}{\sin^2\theta}$$

$$\frac{\partial \theta}{\partial q_{10}} = -\frac{q_{20}}{\sqrt{1-(\dot{q}_1\cdot\dot{q}_2)^2}} \quad \frac{\partial \theta}{\partial q_{20}} = -\frac{q_{10}}{\sqrt{1-(\dot{q}_1\cdot\dot{q}_2)^2}}$$

$$\frac{\partial \theta}{\partial q_{11}} = -\frac{q_{21}}{\sqrt{1-(\dot{q}_1\cdot\dot{q}_2)^2}} \quad \frac{\partial \theta}{\partial q_{21}} = -\frac{q_{11}}{\sqrt{1-(\dot{q}_1\cdot\dot{q}_2)^2}}$$

$$\frac{\partial \theta}{\partial q_{12}} = -\frac{q_{22}}{\sqrt{1-(\dot{q}_1\cdot\dot{q}_2)^2}} \quad \frac{\partial \theta}{\partial q_{22}} = -\frac{q_{12}}{\sqrt{1-(\dot{q}_1\cdot\dot{q}_2)^2}}$$

$$\frac{\partial \theta}{\partial q_{13}} = -\frac{q_{23}}{\sqrt{1-(\dot{q}_1\cdot\dot{q}_2)^2}} \quad \frac{\partial \theta}{\partial q_{23}} = -\frac{q_{13}}{\sqrt{1-(\dot{q}_1\cdot\dot{q}_2)^2}}$$

Using the deflection differential coefficients of equation (13) in error equation (11), the error equation of exterior orientation based on quaternion SLERP model is given by:

$$\left.\begin{aligned} v_x =& k'_{11}\mathrm{d}X_S + k'_{12}\mathrm{d}Y_S + k'_{13}\mathrm{d}Z_S \\ &+ k'_{14}\mathrm{d}q_{10} + k'_{15}\mathrm{d}q_{11} + k'_{16}\mathrm{d}q_{12} + k'_{17}\mathrm{d}q_{13} \\ &+ k'_{18}\mathrm{d}q_{20} + k'_{19}\mathrm{d}q_{21} + k'_{110}\mathrm{d}q_{22} + k'_{111}\mathrm{d}q_{23} \\ &+ yk'_{11}\mathrm{d}\dot{X}_S + yk'_{12}\mathrm{d}\dot{Y}_S + yk'_{13}\mathrm{d}\dot{Z}_S - l_x \\ v_x =& k'_{21}\mathrm{d}X_S + k'_{22}\mathrm{d}Y_S + k'_{23}\mathrm{d}Z_S \\ &+ k'_{24}\mathrm{d}q_{10} + k'_{25}\mathrm{d}q_{11} + k'_{26}\mathrm{d}q_{12} + k'_{27}\mathrm{d}q_{13} \\ &+ k'_{28}\mathrm{d}q_{20} + k'_{29}\mathrm{d}q_{21} + k'_{210}\mathrm{d}q_{22} + k'_{211}\mathrm{d}q_{23} \\ &+ yk'_{21}\mathrm{d}\dot{X}_S + yk'_{22}\mathrm{d}\dot{Y}_S + yk'_{23}\mathrm{d}\dot{Z}_S - l_y \end{aligned}\right\} \tag{15}$$

Where

$$\begin{aligned} k'_{11} &= k_{11} = (a_{1i}f + a_{3i}x)/\bar{Z} & k'_{21} &= k_{21} = a_{2i}f/\bar{Z} \\ k'_{12} &= k_{12} = (b_{1i}f + b_{3i}x)/\bar{Z} & k'_{22} &= k_{22} = b_{2i}f/\bar{Z} \\ k'_{13} &= k_{13} = (c_{1i}f + c_{3i}x)/\bar{Z} & k'_{23} &= k_{23} = c_{2i}f/\bar{Z} \end{aligned}$$

$$k'_{14}=k_{14}\frac{\partial q_{i0}}{\partial q_{10}}+k_{15}\frac{\partial q_{i1}}{\partial q_{10}}+k_{16}\frac{\partial q_{i2}}{\partial q_{10}}+k_{17}\frac{\partial q_{i3}}{\partial q_{10}}$$
$$k'_{15}=k_{14}\frac{\partial q_{i0}}{\partial q_{11}}+k_{15}\frac{\partial q_{i1}}{\partial q_{11}}+k_{16}\frac{\partial q_{i2}}{\partial q_{11}}+k_{17}\frac{\partial q_{i3}}{\partial q_{11}}$$
$$k'_{16}=k_{14}\frac{\partial q_{i0}}{\partial q_{12}}+k_{15}\frac{\partial q_{i1}}{\partial q_{12}}+k_{16}\frac{\partial q_{i2}}{\partial q_{12}}+k_{17}\frac{\partial q_{i3}}{\partial q_{12}}$$
$$k'_{17}=k_{14}\frac{\partial q_{i0}}{\partial q_{13}}+k_{15}\frac{\partial q_{i1}}{\partial q_{13}}+k_{16}\frac{\partial q_{i2}}{\partial q_{13}}+k_{17}\frac{\partial q_{i3}}{\partial q_{13}}$$
$$k'_{18}=k_{14}\frac{\partial q_{i0}}{\partial q_{20}}+k_{15}\frac{\partial q_{i1}}{\partial q_{20}}+k_{16}\frac{\partial q_{i2}}{\partial q_{20}}+k_{17}\frac{\partial q_{i3}}{\partial q_{20}}$$
$$k'_{19}=k_{14}\frac{\partial q_{i0}}{\partial q_{21}}+k_{15}\frac{\partial q_{i1}}{\partial q_{21}}+k_{16}\frac{\partial q_{i2}}{\partial q_{21}}+k_{17}\frac{\partial q_{i3}}{\partial q_{21}}$$
$$k'_{110}=k_{14}\frac{\partial q_{i0}}{\partial q_{22}}+k_{15}\frac{\partial q_{i1}}{\partial q_{22}}+k_{16}\frac{\partial q_{i2}}{\partial q_{22}}+k_{17}\frac{\partial q_{i3}}{\partial q_{22}}$$
$$k'_{111}=k_{14}\frac{\partial q_{i0}}{\partial q_{23}}+k_{15}\frac{\partial q_{i1}}{\partial q_{23}}+k_{16}\frac{\partial q_{i2}}{\partial q_{23}}+k_{17}\frac{\partial q_{i3}}{\partial q_{23}}$$
$$k'_{24}=k_{24}\frac{\partial q_{i0}}{\partial q_{10}}+k_{25}\frac{\partial q_{i1}}{\partial q_{10}}+k_{26}\frac{\partial q_{i2}}{\partial q_{10}}+k_{27}\frac{\partial q_{i3}}{\partial q_{10}}$$
$$k'_{25}=k_{24}\frac{\partial q_{i0}}{\partial q_{11}}+k_{25}\frac{\partial q_{i1}}{\partial q_{11}}+k_{26}\frac{\partial q_{i2}}{\partial q_{11}}+k_{27}\frac{\partial q_{i3}}{\partial q_{11}}$$
$$k'_{26}=k_{24}\frac{\partial q_{i0}}{\partial q_{12}}+k_{25}\frac{\partial q_{i1}}{\partial q_{12}}+k_{26}\frac{\partial q_{i2}}{\partial q_{12}}+k_{27}\frac{\partial q_{i3}}{\partial q_{12}}$$
$$k'_{27}=k_{24}\frac{\partial q_{i0}}{\partial q_{13}}+k_{25}\frac{\partial q_{i1}}{\partial q_{13}}+k_{26}\frac{\partial q_{i2}}{\partial q_{13}}+k_{27}\frac{\partial q_{i3}}{\partial q_{13}}$$
$$k'_{28}=k_{24}\frac{\partial q_{i0}}{\partial q_{20}}+k_{25}\frac{\partial q_{i1}}{\partial q_{20}}+k_{26}\frac{\partial q_{i2}}{\partial q_{20}}+k_{27}\frac{\partial q_{i3}}{\partial q_{20}}$$
$$k'_{29}=k_{24}\frac{\partial q_{i0}}{\partial q_{21}}+k_{25}\frac{\partial q_{i1}}{\partial q_{21}}+k_{26}\frac{\partial q_{i2}}{\partial q_{21}}+k_{27}\frac{\partial q_{i3}}{\partial q_{21}}$$
$$k'_{210}=k_{24}\frac{\partial q_{i0}}{\partial q_{22}}+k_{25}\frac{\partial q_{i1}}{\partial q_{22}}+k_{26}\frac{\partial q_{i2}}{\partial q_{22}}+k_{27}\frac{\partial q_{i3}}{\partial q_{22}}$$
$$k'_{211}=k_{24}\frac{\partial q_{i0}}{\partial q_{23}}+k_{25}\frac{\partial q_{i1}}{\partial q_{23}}+k_{26}\frac{\partial q_{i2}}{\partial q_{23}}+k_{27}\frac{\partial q_{i3}}{\partial q_{23}}$$

The expression of l_x and l_y is as the same as that in equation (11).

In the result of the above linearization equation, the form of the coefficients is fit to program. Comparing with the traditional Euler angle model, it successfully avoids a great deal of computation of trigonometric functions.

3.3 Computation of exterior orientation elements

The error equation (15) can be written in the matrix form.

$$\boldsymbol{V}=\boldsymbol{C}\boldsymbol{\delta}_x+\boldsymbol{l} \tag{16}$$

Where

$$\boldsymbol{V}=[v_x\ v_y]^{\mathrm{T}}$$
$$\boldsymbol{C}=\begin{bmatrix}k'_{11} & k'_{12} & \cdots & k'_{111} & yk'_{11} & yk'_{12} & yk'_{13}\\ k'_{21} & k'_{22} & \cdots & k'_{211} & yk'_{21} & yk'_{22} & yk'_{23}\end{bmatrix}$$
$$\boldsymbol{\delta}_x=[\mathrm{d}X_S\ \mathrm{d}Y_S\ \mathrm{d}Z_S\ \mathrm{d}q_{10}\ \mathrm{d}q_{11}\ \mathrm{d}q_{12}\ \mathrm{d}q_{13}\ \mathrm{d}q_{20}\ \mathrm{d}q_{21}\ \mathrm{d}q_{22}\ \mathrm{d}q_{23}\ \mathrm{d}\dot{X}_S\ \mathrm{d}\dot{Y}_S\ \mathrm{d}\dot{Z}_S]^{\mathrm{T}}$$
$$\boldsymbol{l}=[l_x\ l_y]^{\mathrm{T}}$$

Because of the unit quaternion which is used to describe the attitude, there are two conditions in the error equations.

$$\left.\begin{aligned}q_{10}^2+q_{11}^2+q_{12}^2+q_{13}^2=1\\ q_{20}^2+q_{21}^2+q_{22}^2+q_{23}^2=1\end{aligned}\right\}$$

The two equations also should be linearized, and the linearization equation is given by:

$$q_{10}\mathrm{d}q_{10}+q_{11}\mathrm{d}q_{11}+q_{12}\mathrm{d}q_{12}+q_{13}\mathrm{d}q_{13}+w_1=0$$
$$w_1=(q_{10}^2+q_{11}^2+q_{12}^2+q_{13}^2-1)$$
$$q_{20}\mathrm{d}q_{20}+q_{21}\mathrm{d}q_{21}+q_{22}\mathrm{d}q_{22}+q_{23}\mathrm{d}q_{23}+w_2=0$$
$$w_2=(q_{20}^2+q_{21}^2+q_{22}^2+q_{23}^2-1)$$

The above equations can be written as follow:

$$\boldsymbol{B}_x\boldsymbol{\delta}_x+\boldsymbol{W}=0 \tag{17}$$

Where

$$\boldsymbol{B}_x=\begin{bmatrix}0\ 0\ 0\ q_{10}\ q_{11}\ q_{12}\ q_{13}\ 0\ 0\ 0\ 0\ 0\ 0\ 0\\ 0\ 0\ 0\ 0\ 0\ 0\ 0\ q_{20}\ q_{21}\ q_{22}\ q_{23}\ 0\ 0\ 0\end{bmatrix}$$
$$\boldsymbol{w}=[w_1\ w_2]^{\mathrm{T}}$$

When there are n points, the total error equations is:

$$\left.\begin{aligned}\boldsymbol{V}=\boldsymbol{C}\boldsymbol{\delta}_x+\boldsymbol{l}\\ \boldsymbol{B}_x\boldsymbol{\delta}_x+\boldsymbol{W}=0\end{aligned}\right\} \tag{18}$$

Where $\boldsymbol{V}$ and $\boldsymbol{l}$ are the matrix with $2n\times 1$; $\boldsymbol{C}$ is the matrix with $2n\times 10$; n is the number of ground control points (GCPs).

Supposed the weight matrix of observed value is $\boldsymbol{P}$, we can gain the solution of equation (18) according parameter adjustment with constraints.

$$\boldsymbol{Y}=-\boldsymbol{N}^{-1}\boldsymbol{W}_Y \tag{19}$$

Where

$$\boldsymbol{Y}=\begin{bmatrix}\boldsymbol{\delta}_x\\ \boldsymbol{K}\end{bmatrix},\boldsymbol{N}=\begin{bmatrix}\boldsymbol{C}^{\mathrm{T}}\boldsymbol{P}\boldsymbol{C} & \boldsymbol{B}_x^{\mathrm{T}}\\ \boldsymbol{B}_x & 0\end{bmatrix},\boldsymbol{W}_Y=\begin{bmatrix}\boldsymbol{C}^{\mathrm{T}}\boldsymbol{P}\boldsymbol{C}\\ \boldsymbol{W}\end{bmatrix} \tag{20}$$

When the number of GCPs $n\geq 6$, given the initial value of line and attitude elements $\boldsymbol{\delta}_x^0$, we can obtain the most probable value of the line and attitude elements $\boldsymbol{\delta}_x$ iteratively through equation (19) until that the result is smaller than the tolerance.

3.4 Summary of the algorithm

The complete algorithm works as follows:

(1) Input the base data, including observed value of image points and the ground coordinate of the corresponding GCPs.

(2) Determine the initial values of exterior orientation elements $\boldsymbol{\delta}_x^0$. In this quaternion algorithm, the initial values has not special requirement. We just can give the initial values as $X_{S0}=\bar{X}_{GCP}$, $Y_{S0}=\bar{Y}_{GCP}$, $Z_{S0}=H$, $q_{10}=1$, $q_{11}=q_{12}=q_{13}=0$, $q_{20}=1$, $q_{21}=q_{22}=q_{23}=0$, $\dot{X}_S=\dot{Y}_S=\dot{Z}_S=0$,where $\bar{X}_{GCP}$,$\bar{Y}_{GCP}$ are the average value of GCPs ground coordinate. Then begin the iteration.

(3) Compute exterior orientation elements of every GCP using equation (7) and (9), and calculate the quaternion rotation matrix using equation (1).

(4) Compute the matrix$\boldsymbol{C}$,$\boldsymbol{l}$ and weight matrix $\boldsymbol{P}$ using error equation (16), and estimate value of the least squares prediction $\boldsymbol{\delta}_x$.

(5) Update the exterior orientation elements with formula $\boldsymbol{\delta}_x^1=\boldsymbol{\delta}_x^0+\boldsymbol{\delta}_x$, and check that whether the result $\boldsymbol{\delta}_x$ is less than the tolerance or not. If it is less than the tolerance, the iteration ends, and the result $\boldsymbol{\delta}_x^1$ is the estimation value of the exterior orientation elements. Otherwise, repeat step 3 to step 4 until the result of exterior orientation elements is less than the tolerance.

4. EXPERIMENTS AND RESULTS

The exterior orientation process of line-array CCD images is to obtain the exterior orientation elements of the images using GCPs and their image points. In order to verify the efficiency of this quaternion method, experiments are done on the solution of exterior orientation elements by various methods.

The experiment data used in this paper are two SPOT images (Level 1A) of TangShan area in china: Image_01 and Image_02, which constitute a single stereo. The size of the pixel is 13μm×13μm, the focal length of the camera is 1082 mm, and the size of the image is 6000×6000. The flight height is about 830 000.0 m, the swath width is 60km×60km, and the overlap of these two images exceeds 80%. The ground coordinate uses Gaussian coordinate system, and the longitude of central meridian is 117 degree. The ground altitude difference is 0～500 m.

Figure 2 is the outline of GCPs which is distributed evenly in images. The control points are measured from 1:50,000 topographic maps. For Image_01 and Image_02, 19 control points are selected respectively, with 13 orientation points and 6 checking points. There are 13 homologous points in the two images.

We use the following methods in our experiments.

Method 1: Our algorithm

Method 2: LS estimation (Qian, 1991).

Method 3: General ridge estimation (Guo, 2003).

In order to validate the independence of the initial value of our method, we use the coordinate of GCPs to compute the initial value in our experiment. So, we consider that there is not any priori information of images, and the initial values are as follow: $X_{S0} = \bar{X}_{GCP}$, $Y_{S0} = \bar{Y}_{GCP}$, $Z_{S0} = H$, $q_{10} = 1$, $q_{11} = q_{12} = q_{13} = 0$, $q_{20} = 1$, $q_{21} = q_{22} = q_{23} = 0$, $\dot{X}_S = \dot{Y}_S = \dot{Z}_S = 0$.

In our experiments, we use the analytical method to analyse the precision. The solution precision of exterior orientation elements can be evaluated by the following two checking methods. One is computing the reprojection error. The other is computing ground points coordinate by space intersection, and then calculating the mean square error.

In table 3 and table 4, $\boldsymbol{v}_{ox}$,$\boldsymbol{v}_{oy}$,$\boldsymbol{v}_{oX}$,$\boldsymbol{v}_{oY}$,$\boldsymbol{v}_{oZ}$are the precision (mean square error) for the image coordinates x, y and the ground coordinates X,Y,Z of orientation points respectively; while $\boldsymbol{v}_{cx}$,$\boldsymbol{v}_{cy}$,$\boldsymbol{v}_{cX}$,$\boldsymbol{v}_{cY}$,$\boldsymbol{v}_{cZ}$ are the precision (mean square error) for the image coordinates x,y and the ground coordinates X,Y,Z of the checking points respectively.

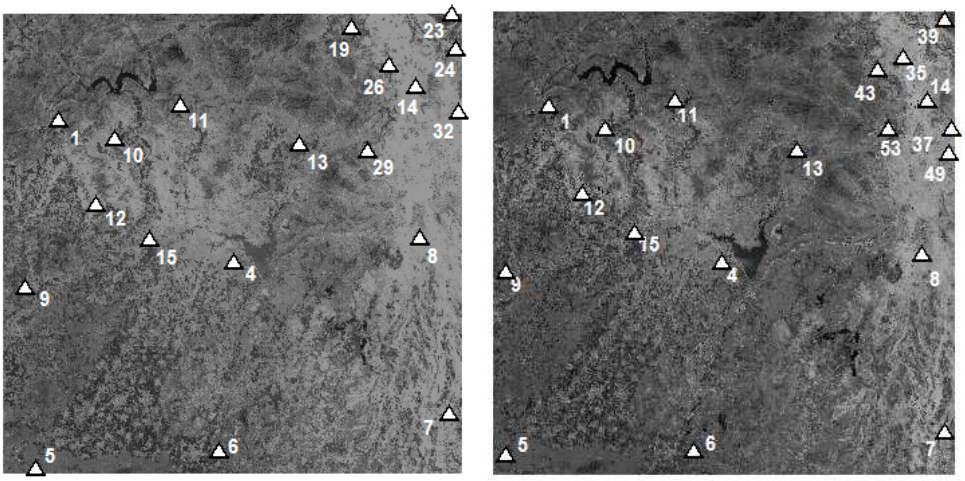

(a) (b)

Figure 2. The outline of GCPs : (a) Image_01 (b) Image_02

Method	Mean Square error for the coordinates of orientation points					Mean Square error for the coordinates of checking points				
	$\boldsymbol{v}_{ox}$/Pixel	$\boldsymbol{v}_{oy}$/Pixel	$\boldsymbol{v}_{oX}$/m	$\boldsymbol{v}_{oY}$/m	$\boldsymbol{v}_{oZ}$/m	$\boldsymbol{v}_{cx}$/Pixel	$\boldsymbol{v}_{cy}$/Pixel	$\boldsymbol{v}_{cX}$/m	$\boldsymbol{v}_{cY}$/m	$\boldsymbol{v}_{cZ}$/m
Method 1	0.91	0.87	7.68	10.16	17.08	1.35	1.22	13.40	10.13	21.38
Method 2	1.68	1.58	20.03	22.87	84.92	1.90	1.82	25.87	31.89	96.32
Method 3	0.91	0.93	9.23	14.92	41.94	1.61	1.12	20.79	13.43	63.35

Table 3. Orientation precision of Image_01 under various methods

Method	Mean Square error for the coordinates of orientation points					Mean Square error for the coordinates of checking points				
	$\boldsymbol{v}_{ox}$/Pixel	$\boldsymbol{v}_{oy}$/Pixel	$\boldsymbol{v}_{oX}$/m	$\boldsymbol{v}_{oY}$/m	$\boldsymbol{v}_{oZ}$/m	$\boldsymbol{v}_{cx}$/Pixel	$\boldsymbol{v}_{cy}$/Pixel	$\boldsymbol{v}_{cX}$/m	$\boldsymbol{v}_{cY}$/m	$\boldsymbol{v}_{cZ}$/m
Method 1	0.89	0.91	7.68	10.16	17.08	1.50	1.27	13.40	10.13	21.38
Method 2	1.52	1.58	20.03	22.87	84.92	1.71	1.49	25.87	31.89	96.32
Method 3	1.08	1.59	9.23	14.92	41.94	1.25	2.14	20.79	13.43	63.35

Table 4. Orientation precision of Image_02 under various methods

From table 3 and table 4, it can be seen that the quaternion algorithm can obtain exterior orientation elements successfully. The plane positioning precision is about 1 GSD, and better than that of the LS estimation and the general ridge estimation. However, the height positioning precision is less admirable, we think that the main reason is the influence of the measure error for GCPs. Of course, due to the initial values which gained by GCPs only, the positioning precision of the LS estimation and the general ridge estimation is not very high, and that show our algorithm is independence on the initial values. At the same time, special calculation measures are not required in the computing process, which shows that the influence of ill-posed problem is weaken effectively by this quaternion algorithm. However, because the attitude quaternions which used to describe the exterior orientation elements of the first and the last scan line of a line-array CCD image are unknown numbers, the redundant parameters is also exited, and deep researches are needed.

5. CONCLUSIONS

Line-array CCD Images are widely used in target positioning of remote sensing imagery. However, the orientation parameters of traditional linearization collinear equation are highly correlated because of such factors as big flying height, small angle of coverage, narrow light beam and so on. Thus, it is fairly difficult to gain steady and precise solutions. We use quaternion to describe the attitude elements in this paper, and then build a model of exterior orientation elements. It can obtain reliable and precise positioning results. Compared with traditional solution methods, it successfully avoids a great deal of computation of trigonometric functions and the potential unstable factors, and hasn't special requirement for initial values. So it is quite suit for exterior orientation of line-array CCD Images without good initial values. At present, there are many space photographs without ephemeris data, and how to use these images to position is a challengeable work in photogrammetry. The quaternion algorithm in this paper provides a method for finding the exterior orientation elements of these line-array CCD images, and provides precise initial values for consequent applications.

REFERENCE

Amnon krupnik. 2000. Accuracy assessment of automatically derived digital elevation models from spot image. *Photogrammetric Engineering and Remote Sensing*. 66(8), pp.1017-1023.

Fraser C S, Hanley H B, Yamakawa T. 2002, Three-Dimensional Geopositioning Accuracy of Ikonos Imagery. *Photogrammetric Record*, 17(99), pp.465-479.

Fuzhen Zhang. 1997. Quaternions and Matrices of Quaternions .*Linear Algebra and its Applications.* 252, pp.21-57.

Gui Qingming, Guo Haitao, Guo Jianfeng, et al. 2003. Computing the Exterior Orientation Elements of One-line Scanner Satellitic Imagery By Using Principal Component Estimation, *Remote Sensing Technology and Application*, 18(1), pp.14-18. (In Chinese.)

Guo Haitao, Zhang Baoming, Gui Qingming. 2003. Application of generalized ridge estimate to computing the exterior orientation elements of satellite linear array scanner imagery, *Geomatics and Information Science of Wuhan University*, 28(4). pp.444-447. (In Chinese.)

Jiang Gang-wu, Jiang Ting, Wang Yong, et al. 2007,5. Space Resection Indepdent of Initial Value Based on Unit Quaternions. *Acta Geodaetica et Cartographica Sinica*, 36(2), pp.169-175. (In Chinese.)

Katiyar S.K, Onkar Dikshit, Krishna Kumar. 2003. Linear pushbroom model for IRS-1C/D satellite imaging geometry. *IEEE International of Geoscience and Remote Sensing Symposium*, vol 6, pp.3613-3615.

Liu Jun, Wang Donhong, Zhang Yongsheng. 2008. Triangulation of Airborne Three-Line Images using Unit Quaternion. *The International Archives of the Photogrammetry Remote Sensing and Spatial Information Sciences.* Beijing, China Vol. XXXVII. Part B1. pp.573-578.

Okamoto A, Ono T, et al. 1999. Geometric Characteristics of Alternative Triangulation Models for Satellite Imagery. *ASPRS 1999 Aunual Conference Proceedings*. Oregon., pp. 64-72.

Qian Zhengbo, Liu Jingyu, Xiao Guochao. 1991. *Space Photogrammetry*. Publishing House of Surveying and Mapping. Beijing. (In Chinese.)

Rajiv Gupta, Richard I. Hartley, 1997. Linear pushbroom cameras, *IEEE Transactions on Pattern Analysis and Machine Intelligence*, vol. 19, pp. 963-975.

Wang Tao, Zhang Yan, Xu Qing, et al. 2005, A New Method for Linear Pushbroom Imagery Exterior Orientation. *Acta Geodaetica et Cartographica Sinica*, 34(1), pp.35-39. (In Chinese.)

Wang Yong, Jiang Ting, Jiang Gangwu, et al. 2007, Space Resection of Single Image Based on the Description of Unit Quaternions . *Journal of Zhenzhou Institute of Surveying and Mapping*. 24(2), pp.133-135. (In Chinese.)

Wang Zhizhuo. 1979. *The Theory of Photogrammetry*, Publishing House of Surveying and Mappin. Beijing.

Zhang Yongsheng, Gong Danchao. 2004. *Application of high resolution remote sensing satellites*, Publishing House of Science. Beijing,. (In Chinese.)

ACKNOWLEDGEMENTS

This work is supported by the National Natural Science Foundation of China (No. 40901246).